A robust complex local mean decomposition method with self-adaptive sifting stopping

CanYu Mo,[1,2] QianQiang Lin[2,✉], YuanDuo Niu,[1,2] and HaoRan Du[1,2]

[1]*Xi'an Electronic Engineering ResearchInstitute, Xi'an, China*
[2]*College of Electronic Science, National University of Defense Technology, Changsha, China*
✉Email: even_qqlin@nudt.edu.cn

Targets with rotating components generate micro-motion (MM) modulation effect in addition to the main body. Extracting MM parameters is challenging due to interference from the target's main body, necessitating the separation of modulation signals. This letter proposes a robust complex local mean decomposition (RCLMD) method with self-adaptive sifting stopping, aiming at the problem of component redundancy due to multiple iterations during break and the loss of modulation components during the separation process. The proposed method sets the objective function and self-adaptive stopping criterion, combined with the modulation signal characteristics, enhancing the accuracy and efficiency of MM component extraction. Simulation experiments indicate that at a low signal-to-noise ratio (SNR) of 3 dB, the separation effect of RCLMD is still 14.72% higher than that of the conventional complex local mean decomposition (CLMD) method, and the separation efficiency is improved by 54.92%. Furthermore, the measured radar signals verify the effectiveness of the proposed method in real scenarios.

Introduction: The vibration or rotation outside the target main body, is a phenomenon called the micro-Doppler (m-D) effect [1–3]. Particularly for low-altitude targets, micro-motion (MM) phenomena are predominantly attributed to rotating components, such as helicopter blades. These MM modulations are distinct for different targets, making them crucial for target identification and classification. Extracting target-specific parameter information, especially the modulation details of rotating parts, is imperative for characterizing MM parameters [4, 5]. Nevertheless, when the body echo signal is powerful, it can be challenging to accurately obtain the rotating component's parameter information. Consequently, it is necessary to separate the rotating component echo and the body echo according to their echo characteristics.

Time-frequency analysis methods have demonstrated considerable efficacy in separating MM modulation signals of low-altitude targets, as evidenced in recent studies [6, 7]. A notable example is the empirical mode decomposition (EMD) method [8], which is mainly used for MM signal separation. In comparison, the local mean decomposition (LMD) method [9] yields product function (PF) components, each bearing significant physical relevance. This relevance provides a more accurate reflection of the original signal's intrinsic characteristics, thereby enhancing the analysis of modulated signals. However, a limitation of the LMD method is its phase information loss due to the necessity of adopting the modal value of echoes. Addressing this, Park et al.[10] evolved the actual signal LMD method to cater to complex signals. They introduced the complex local mean decomposition (CLMD) method, which adaptively decomposes echo signals into complex PF components of varying frequencies. This advancement facilitates a more nuanced analysis of MM modulated signals, effectively separating rotating parts from target echo signals.

End effect and mode mixing problems are the two main factors limiting the performance of the CLMD method. Appropriate parameter choices for boundary conditions, envelope estimation, and sifting-stopping criteria can mitigate these limitations[11]. Boundary conditions and envelope estimation are the two main research hotspots in the last decade, while the sifting stopping criterion has not received enough attention so far. Smith [12] has defined the principle of sifting stopping criterion. However, the principle could be better implemented with inaccurate signals. Xu et al [13]. have introduced the orthogonality criterion on this basis and transformed the principle of sifting stopping criterion into a method of practical expression. Nonetheless, a critical limitation of these methods is their reliance on pre-specified thresholds, which precludes the possibility of self-adaptive signal decomposition.

Considering this issue, this letter proposes a novel approach: the robust complex local mean decomposition (RCLMD) method with a self-adaptive sifting stopping. An objective function related to the characteristics of the target signal is defined, based on which a self-adaptive stopping iteration mechanism is proposed to determine the optimal number of sifting iterations automatically. Finally, based on the RCLMD method and the CLMD method, the separation ability and efficiency under simulation and measured data is verified, which proves the effectiveness of the proposed method. This advancement holds considerable practical significance.

m-D modulation model: A single rotating blade usually consists of multiple scattering centers for rotary-wing targets such as helicopters. That is, The overall echo of a target with a rotating component can be considered as a linear superposition of the echo components of the k scattering centers, which can be expressed as the modulated echo complex vector shown in equation (1) below:

$$s(t) = \sum_{k=1}^{P} \sigma_k \exp\left(j\psi_k(t)\right) = \sum_{k=1}^{P} \sigma_k \exp\left[j\omega_0\left(t - \frac{2r_i(t)}{c}\right)\right] \quad (1)$$

where σ_k represents the amplitude of the k-th scattering center, $\psi_k(t)$ means the phase of the k-th scattering center, $\omega_0 = 2\pi f_0, f_0$ is the carrier frequency of the radar, and $r_i(t)$ is the distance of the k-th scattering center from the radar at time t.

Based on the MM modulation signal model, it is recognized that the radial movement of any scatterer on a rotating part relative to the radar induces alterations in both amplitude and phase of the echo signal. This dynamic results in the generation of MM modulation components that are external to the main body signal.

Proposed method: CLMD method aims to extract a set of "best-fit" PF components of pure FM and envelope signals. Still, the end effect and mode-mixing problems can limit its decomposition performance. To alleviate this limitation, this letter proposes RCLMD method based on the sifting stopping criterion, the basic process is shown in Figure 1.

The self-adaptive sifting stopping criterion proposed in this letter aims to achieve robust decomposition around the following two objectives:

1. Determine the sifting-stopping objective function in combination with the modulated signal characteristics.
2. Adaptively stop the sifting according to the iterative update value of the objective function.

The following are the implementation steps of RCLMD method with self-adaptive sifting stopping.

Step 1: The continuous complex signal $s(t)$ is sampled at sampling frequency f_s to obtain the discrete complex signal $s_{i,k}(n)$, where i denotes the serial number of the product function, k denotes the serial number of the iteration in the decomposition process, and $n = 1, 2, \cdots, N$ denotes the number of sampling points. Let $p_0(n)$ and $p_{\pi/2}(n)$ be the real and imaginary parts of the discrete complex signal $s_{i,k}(n)$, respectively:

$$p_0(n) = \text{Re}\left(e^{-j0} s_{i,k}(n)\right) \quad (2)$$

$$p_{\pi/2}(n) = \text{Re}\left(e^{-j\pi/2} s_{i,k}(n)\right) \quad (3)$$

Assumptions $\tilde{m}_{0(i,k)}(n)$ and $\tilde{a}_{0(i,k)}(n)$ represent the smoothed mean and envelope of $p_0(n)$; $\tilde{m}_{\pi/2(i,k)}(n)$ and $\tilde{m}_{\pi/2(i,k)}(n)$ represent the smoothed mean and envelope of $p_{\pi/2}(n)$.

Step 2: The smoothed mean function $M_{i,k}(n)$ of the complex signal can be obtained from the smoothed mean functions of the real and imaginary parts of the signal:

$$M_{i,k}(n) = mc_{0(i,k)}(n) + mc_{\pi/2(i,k)}(n) \quad (4)$$

where the real part of the smoothed mean function is denoted as $mc_{0(i,k)}(n) = e^{j0}\tilde{m}_{0(i,k)}(n)$ and the imaginary part as $mc_{\pi/2(i,k)}(n) = e^{j\pi/2}\tilde{m}_{\pi/2(i,k)}(n)$.

Step 3: Separate the complex smoothed mean function $M_{i,k}(n)$ from the original complex signal $s_{i,k}(n)$:

$$H_{i,k}(n) = s_{i,k}(n) - M_{i,k}(n) \quad (5)$$
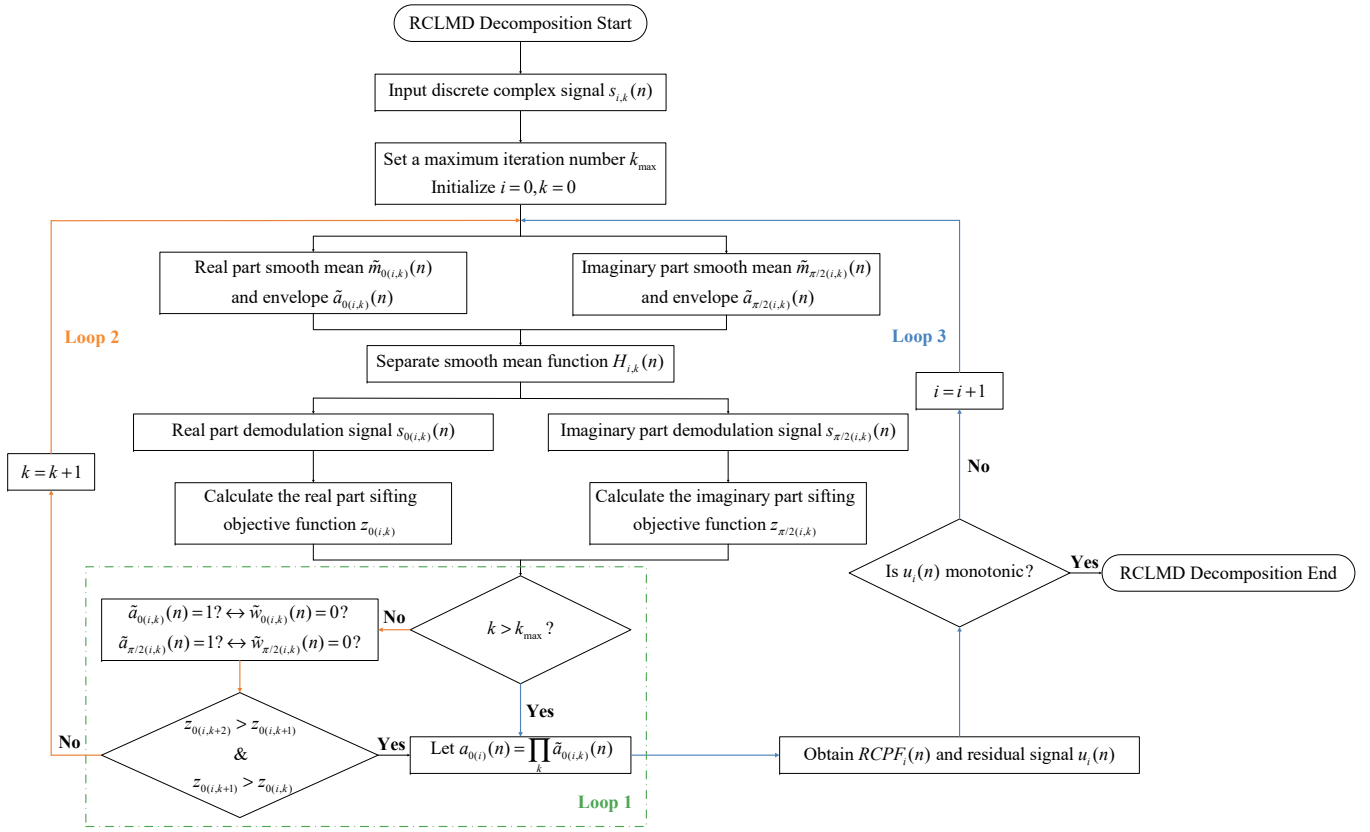
Fig. 1 *Robust complex local mean decomposition method with self-adaptive sifting stopping process*

Step 4: The real and imaginary parts of the complex signal can be demodulated separately to obtain demodulated signals of $s_{\pi/2(i,k)}(n)$ and $s_{\pi/2(i,k)}(n)$.

$$s_{0(i,k)}(n) = \mathrm{Re}(e^{j0}H_{i,k}(n))/\tilde{a}_{0(i,k)}(n) \quad (6)$$

$$s_{\pi/2(i,k)}(n) = \mathrm{Re}(e^{-j\pi/2}H_{i,k}(n))/\tilde{a}_{\pi/2(i,k)}(n) \quad (7)$$

where loop 1 stops on the condition that the demodulated signal is a pure FM signal, i.e., to determine whether $\tilde{a}_{0(i,k)}(n)$ and $\tilde{a}_{\pi/2(i,k)}(n)$ are equal to 1.

Based on this principle, the proposed method defines $\tilde{w}_{0(i,k)}(n) = \tilde{a}_{0(i,k)}(n) - 1$ and $\tilde{w}_{\pi/2(i,k)}(n) = \tilde{a}_{\pi/2(i,k)}(n) - 1$ as the real and imaginary parts of the zero-mean envelope signal. It transforms the selection of the number of sifting stop iterations into a judgment of the value of the sifting objective function by loop 2. Combined with the characteristics of the modulated signal, the sifting objective function is designed as follows:

$$z_{0(i,k)} = SD(\tilde{w}_{0(i,k)}(n)) + |EK(\tilde{w}_{0(i,k)}(n))| \quad (8)$$

$$z_{\pi/2(i,k)} = SD(\tilde{w}_{\pi/2(i,k)}(n)) + |EK(\tilde{w}_{\pi/2(i,k)}(n))| \quad (9)$$

The standard deviation $SD = \sqrt{\dfrac{1}{N}\sum_{n=1}^{N}\left(\tilde{w}_{0(i,k)}(n) - \overline{\tilde{w}_{0(i,k)}}\right)^2}$ char-

acterizes the degree of discretization of the zero-mean envelope signal at each iteration of the loop, from which the smoothness of the signal is judged.

Excess kurtosis $EK = \dfrac{\dfrac{1}{N}\sum_{n=1}^{N}\left(\tilde{w}_{0(i,k)}(n) - \overline{\tilde{w}_{0(i,k)}}\right)^4}{\left[\dfrac{1}{N}\sum_{n=1}^{N}\left(\tilde{w}_{0(i,k)}(n) - \overline{\tilde{w}_{0(i,k)}}\right)^2\right]^2} - 3$ indicates

a measure of the possible local spikiness of the whole signal, excluding the minimum 3 poles required for decomposition.

Step 5: In each iteration, the objective function values $z_{0(i,k)}$ and $z_{\pi/2(i,k)}$ can be calculated by their definitions in the equation. The decision is made based on the objective function results of the last three iterations of the self-adaptive stopping process of the proposed screening

iteration. Taking the real part of the signal as an example, if $z_{0(i,k+2)} > z_{0(i,k+1)}$ and $z_{0(i,k+1)} > z_{0(i,k)}$, then the screening process stops, and the corresponding result $\tilde{a}_{0(i,k)}(n)$ at the k-th iteration is returned; otherwise, the screening process continues until the number of iterations reaches a predefined value k_{max}, which represents the maximum number of iterations allowed in each screening process.

Step 6: The real and imaginary envelope signals of the complex signal are obtained by multiplying all the smoothed envelope estimation functions generated during the iteration process, respectively:

$$a_{0(i)}(n) = \prod_k \tilde{a}_{0(i,k)}(n) \quad (10)$$

$$a_{\pi/2(i)}(n) = \prod_k \tilde{a}_{\pi/2(i,k)}(n) \quad (11)$$

The robust complex product function can be expressed as:

$$\mathrm{RCPF}_i(n) = a_{0(i)}(n)s_{0(i,k)}(n)e^{j0} + a_{\pi/2(i)}(n)s_{\pi/2(i,k)}(n)e^{j\pi/2} \quad (12)$$

At this point, the residual signal $u_i(n)$ can be represented as:

$$u_i(n) = s_{i,k}(n) - \mathrm{RCPF}_i(n) \quad (13)$$

Determine whether the residual signal $u_i(n)$ exists in an oscillatory mode and process it through loop 3 until the residual signal doesn't exist in an oscillatory mode. The final residual signal is indicated by $u(n)$.

Step 7: A complete representation of the complex local mean decomposition of the signal is obtained by summing all complex product functions and the final residual signal:

$$x(n) = \sum_i \mathrm{RCPF}_i(n) + u(n) \quad (14)$$

Simulation and real implementation results: In this section, the validity of the proposed method is verified with simulated and measured data.

Firstly, in order to quantitatively measure the separation effect, simulation modulated signals (simulation parameters are set similarly to measured data) are used to analyze the comparative test between the RCLMD and CLMD methods under the same hardware conditions

(CPU: i5-11300H@3.10GHz, Memory: 16GB) for Monte Carlo 100 simulations.

The effect ratio of echo m-D separation can be defined as:

$$Per = \frac{\sum_{r} |\text{Modulation}(r)|}{\sum_{r} |\text{Total}(r)|} \quad (15)$$

where r is the number of rotating paddles, $\text{Total}(r)$ denotes the sum of the energies of the scattering points of the rotating components of the original echo, $\text{Modulation}(r)$ denotes the energy of the signal of the scattering points of the rotating components obtained by separation.
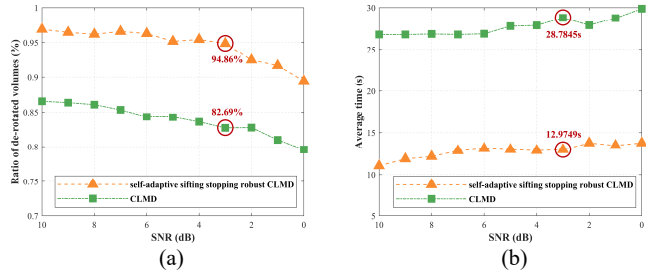
Fig. 2 *Monte Carlo simulations compare the separation effect and time consumption of RCLMD and CLMD (a) Comparison of MM separation effect (b) Comparison of MM separation time consuming*

From Figure 2, it can be seen that RCLMD method can separate the modulation components more efficiently and with better separation results compared to the CLMD method. The advantage of the RCLMD method is more evident under the condition of low SNR. When the SNR is 3dB, the separation effect of the RCLMD method is 14.72% better than that of the CLMD method, and the separation efficiency is 54.92% higher.

Secondly, the validity of this algorithm is verified by measured data. The measured target is the civil aviation helicopter Robinson R44, which has a pair of rotating blades on the top with a rotational speed of 6.8 Hz. The radar-transmitting waveforms of the data acquisition scenario are linear frequency modulation pulse signals and relevant parameters are as follows: the carrier frequency is 3.133 GHz, the bandwidth is 120 MHz, the pulse width is 2.084 μs, the pulse repetition frequency is 3.720 kHz, the distance dimension sampling points are 8192, and the sampling frequency is 20 kHz.
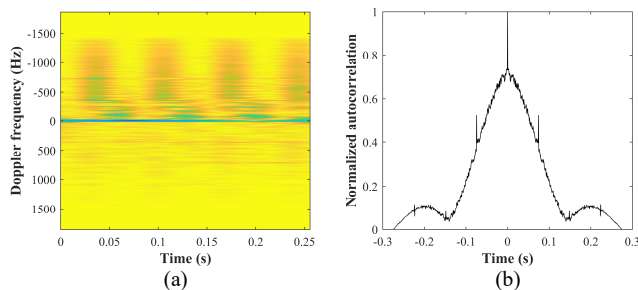

Fig. 3 *Pre-separation overall echo (a) overall echo time-frequency spectrum (b) overall echo autocorrelation*

Figure 3a displays the time-frequency analysis of the overall echo, captured from 1024 pulses in the target's 1841st distance cell, before separation process. It shows the modulation components generated by the paddles during the target's hovering state, which are evident on both sides of the dominant echo. The asymmetry in positive and negative frequencies arises from the disparate scattering areas encountered during the approach and retreat phases, attributable to the physical structure of the target paddles.

The raw echo autocorrelation of range cell 1841, calculated to reveal more about the rotating components, is depicted in Figure 3b. The analysis shows that accurately estimating the frequency of these components

is problematic, primarily due to the superimposition of the m-D effects from the rotating components over the main body echoes.
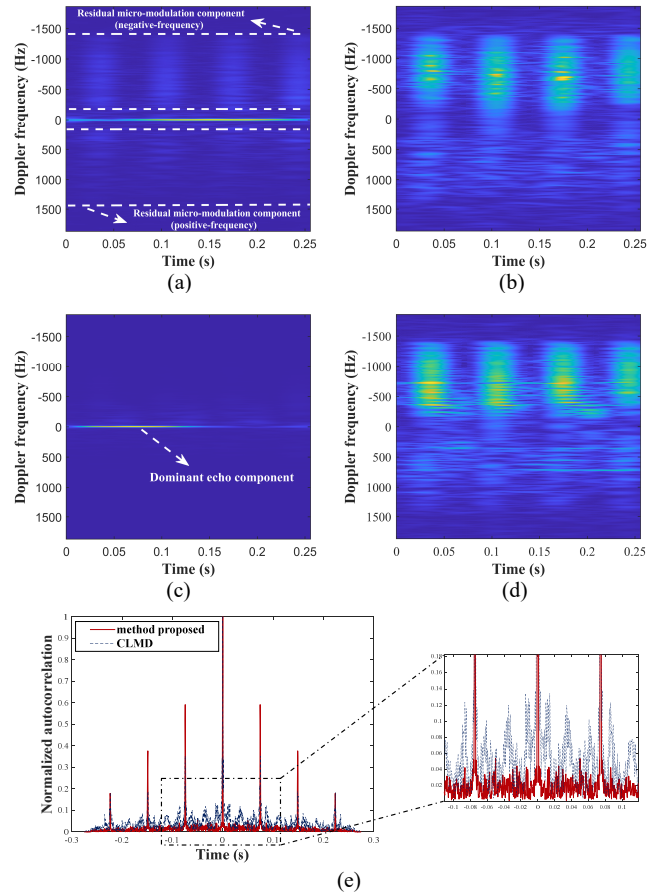
Fig. 4 *Comparison of MM separation effect for measured data (a) Time-frequency spectrum of main body after CLMD separation (b) Time-frequency spectrum of modulation component after CLMD separation (c) Time-frequency spectrum of main body after RCLMD method separation (d) Time-frequency spectrum of modulation component after RCLMD method separation (e) Comparison of autocorrelation function of modulation component*

According to Figure 4a-d, there are still more residual components in the main body component after the separation of the CLMD method. In contrast, almost no modulation component remains in the main body after separation by the RCLMD method, and the modulated echo energy of the rotating part is uniformly distributed on both sides of the main body frequency. Figure 4e shows the autocorrelation function of the modulated echo after separating the MM modulation components of the two methods. The autocorrelation function of the proposed method is smoother, i.e., the periodicity of the rotating part is more apparent. The rotational period (i.e., the time interval between the point of the maximum peak and the point of the second-largest peak) can be estimated from the autocorrelation to be 0.074s. The corresponding rotational frequency is estimated to be 13.514Hz, which is in accordance with the target actual parameters (the actual rotational frequency is the product of blade speed and number of blades: $6.8 \times 2 = 13.6$Hz).

Conclusion: To prevent component redundancy from multiple iterations and loss of modulated components during the separation of target's rotating parts. This letter proposes the RCLMD method with self-adaptive sifting stopping. The method employs an objective function designed for sifting stopping, integrating modulated signal characteristics to efficiently and accurately separate components. Both simulation and empirical data validate its effectiveness. Consequently, the RCLMD with self-adaptive sifting stopping demonstrates enhanced robustness in MM modulation signal separation, which is of great significance for the subsequent application areas with target feature extraction of rotating parts.

References

1. Tian, X. ed.: Fusion recognition of space targets with micromotion. *Electron. Syst.* **58**(4), 3116–3125 (2022)
2. Han, L.X., Feng, C.Q.: Parameter Estimation for Precession Cone-Shaped Targets Based on Range-Frequency-Time Radar Data Cube. *Remote Sens.* **14**(7), 1548 (2022)
3. Wang, H.B. ed.: Micro-Doppler effect removal in inverse synthetic aperture radar imaging based on UNet. *Electron. Lett.* **59**(9), 12814 (2023)
4. Shao, D. ed.: Noise suppression of distributed acoustic sensing vertical seismic profile data based on time–frequency analysis. *Acta Geophys.* **70**, 1539–1549 (2022)
5. Han, L.X., Feng, C.Q.: High-Resolution Imaging and Micromotion Feature Extraction of Space Multiple Targets. *IEEE Trans. Aerosp. Electron. Syst.* **59**(5), 6278–6291 (2023)
6. Xu, X. ed.: A Method for the Micro-Motion Signal Separation and Micro-Doppler Extraction for the Space Precession Target. *IEEE Access.* **8**, 130392–130404 (2020).
7. Zeng, Z.X. ed.: Automatic Arm Motion Recognition Based on Radar Micro-Doppler Signature Envelopes. *IEEE Sens. J.* **20**(22), 13523–13532 (2020).
8. Zhao, Y., Su, Y.: The Extraction of Micro-Doppler Signal With EMD Algorithm for Radar-Based Small UAVs' Detection. *IEEE Trans. Instrum. Meas.* **69**(3), 929–940 (2020).
9. Dai, T. ed.: Extraction of Micro-Doppler Feature Using LMD Algorithm Com-bined Supplement Feature for UAVs and Birds Classification. *Remote Sens.* **14**(9), 2196 (2022)
10. Yuan, B. ed.: Micro-Doppler Analysis and Separation Based on Complex Local Mean Decomposition for Aircraft With Fast-Rotating Parts in ISAR Imaging. *IEEE Trans. Geosci. Electron.* **52**(2), 1285–1298 (2014)
11. Li, Y.B. ed.: A new rotating machinery fault diagnosis method based on improved local mean decomposition. *IEEE Trans. Circuits Syst.* **46**(C), 201–214 (2015)
12. Smith, J.S.: The local mean decomposition and its application to EEG percep-tion data. *J. R. Soc. Interface.* **2**, 443–454 (2005)
13. Xu, Y. ed.: Optimized LMD method and its applications in rolling bearing fault diagnosis. *Meas. Sci. Technol.* **30**(12), 125017 (2019)